J Mater Sci (2021) 56:19244–19252

Metals & corrosion

Low temperature super ductility and threshold stress of an ultrafine-grained Al–Zn–Mg–Zr alloy processed by equal-channel angular pressing

Bálint Boldizsár[1], Péter Jenei[1], Anwar Q. Ahmed[1], Maxim Yu. Murashkin[2,3], Ruslan Z. Valiev[2,3], and Nguyen Q. Chinh[1,*]

[1] *Department of Materials Physics, Eötvös Loránd University, Pázmány Péter sétány 1/A., Budapest 1117, Hungary*
[2] *Institute of Physics of Advanced Materials, Ufa State Aviation Technical University, 12 K. Marx St., Ufa, Russia 450008*
[3] *Laboratory for Mechanics of Bulk Nanomaterials, Saint Petersburg State University, 28 Universitetskypr., Peterhof, St. Petersburg, Russia 198504*

Received: 3 June 2021
Accepted: 13 September 2021
Published online: 23 September 2021

ABSTRACT

Low temperature tensile and impression creep tests were carried out on an ultrafine-grained 7xxx series Al–4.8Zn–1.2 Mg–0.14Zr (wt%) alloy, which can be deformed for maximum elongation of about 200% at 150 °C. The characteristics of the deformation process, such as the strain rate sensitivity (SRS) and activation energy (Q) were determined by considering also the effect of threshold stress. Relatively high SRS of ~ 0.35 and low activation energy of ~ 92 kJ/mole were obtained, confirming the super ductility of the investigated ultrafine-grained alloy in the low temperature region between 140 and 160 °C.

Handling Editor: P. Nash.

Address correspondence to E-mail: chinh@metal.elte.hu

https://doi.org/10.1007/s10853-021-06527-4

GRAPHICAL ABSTRACT

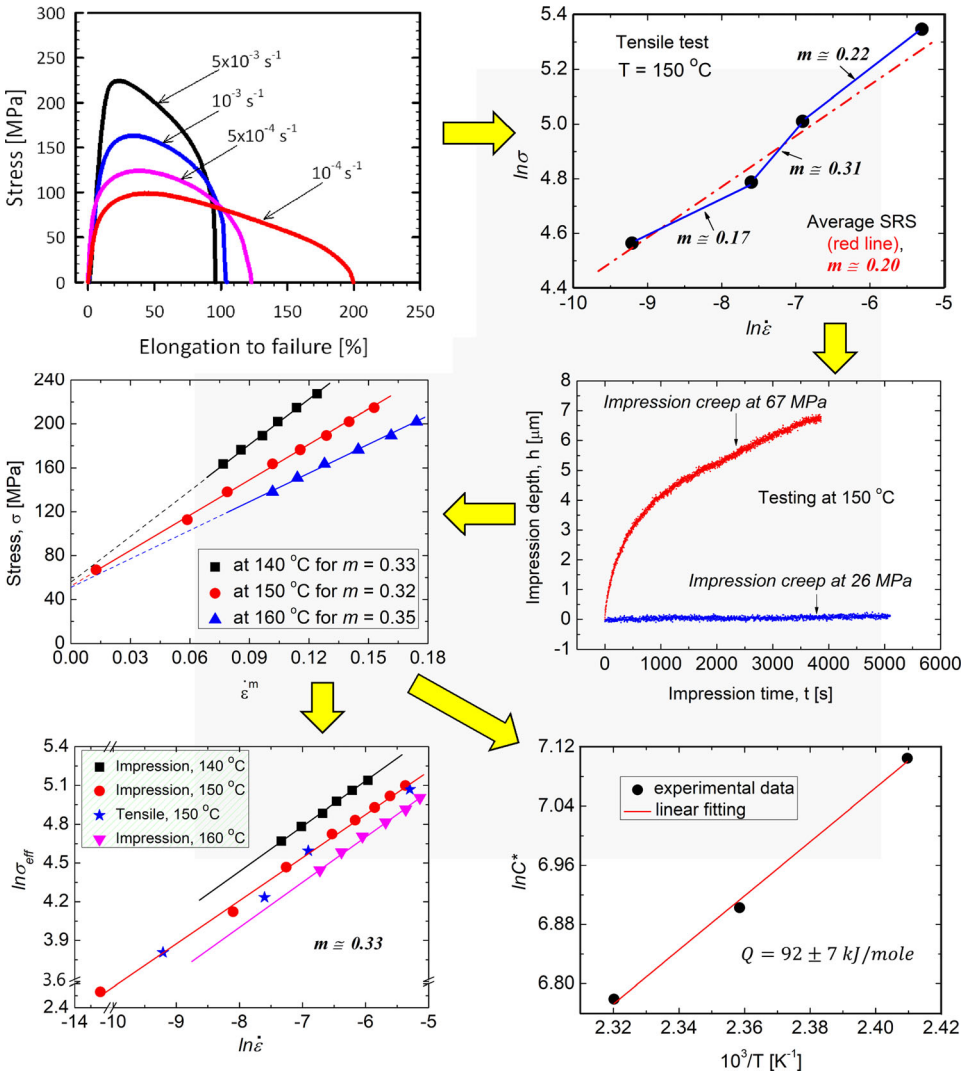

Introduction

Age-hardenable materials, such as Al–Zn–Mg alloys (7xxx series) are widely investigated due to their technological and practical importance, as these alloys are ductile at high temperatures and having high strength at low temperatures. In general, the conventional coarse-grained AlZnMg alloys have very poor ductility at low temperatures, under $0.5T_m$, where T_m is the melting point. In the case of Al alloys, the value of $0.5T_m$ is about 473 K or 200 °C. In the last two decades, by applying severe plastic deformation (SPD), such as equal-channel angular pressing (ECAP) [1–6] and high-pressure torsion (HPT) [7–11] techniques, several conventional Al–Zn and Al–Zn–Mg alloys have been ultrafine-grained (UFG) so that the average grain size was decreased significantly, typically down to the ultrafine region between 100 and 500 nm. The UFG structure then, in general, enhances both the strength of the materials by the well-known Hall–Petch effect [12, 13] and the role of the grain boundary sliding even at room temperature [6, 10, 14, 15]. As a consequence, for instance, the

ductility and the corresponding strain rate sensitivity of some UFG Al–Zn alloys at room temperatures were significantly improved, showing the super ductility of higher than 150% and unusually high SRS above 0.25 [10, 15].

In general, the conventional method of the investigation of ductility is the tensile test, which requires many specimens and relatively expensive equipment. It is well-established that in order to study the plastic behavior of the samples, the investigation can be focused on the strain rate sensitivity because this parameter correlates unambiguously to the ductility [16–18]. Furthermore, the characteristics of plastic deformation, particularly for superplastic materials, can be determined by other alternative methods, for example, by impression creep test [19–31], which method was first suggested and developed by Chu and Li [19]. For this test, a small amount of testing material can be used, and the machining of the samples is simple.

In this work, the deformation characteristics, such as SRS and activation energy of an ECAP-processed, ultrafine-grained Al–Zn–Mg–Zr alloy are studied by using tensile and impression creep tests, in a low temperature region under 170 °C, where the UFG structure remains thermally stable. In order to obtain realistic values for these characteristics, the experimental data were analyzed in terms of an effective stress, σ_{eff}, which is the difference between the applied stress, σ and a threshold stress, σ_0. This concept has been already successfully applied for describing the deformation process of several superplastic materials [22, 32, 33].

Materials and methods

Sample-processing

An alloy with the composition of Al–4.8%Zn–1.2%Mg–0.14%Zr (wt%) was processed by casting. The as-cast material was homogenized in air at 470 °C for 8 h, and then hot extruded to a sheet of 10×50 mm^2 cross section at 380 °C. Cylindrical billets with 10 mm in diameter and 70 mm in length were fabricated from the extruded sheet, then subjected to solution heat-treatment at 470 °C for 30 min and water-quenched to receive a supersaturated solid solution. The billets then have been processed by the ECAP technique at room temperature (RT), in four passes, following route (BC). It is noted that in order to avoid break due to the strengthening effect of Guinier–Preston (GP) zones [3], the samples were started to be processed by ECAP within 15 min following the quenching. More details about the sample can be found in the previous work [4].

Figure 1 shows the microstructure of the investigated ECAP-processed sample. The transmission electron microscopy (TEM) image of Fig. 1a demonstrates the ultrafine-grained (UFG) structure of the sample. It has been shown in the previous work that the average grain size of this UFG structure is about 260 ± 30 nm. Furthermore, there are smaller precipitates having a size of ~ 2 nm and larger particles with the diameter of about 10–20 nm inside the grains, as shown in Fig. 1b. The corresponding energy-disperse X-ray spectroscopy (EDS) elemental maps for Al, Zn, Mg, and Zr can be seen in Fig. 1c–f, respectively. The larger particles are Al_3Zr and η–phase $MgZn_2$, and the smaller ones are Guinier–Preston (GP) zones [4]. It has also been shown in the previous work [4] that the microstructure of this sample remains ultrafine-grained in the low temperature region between 120 and 170 °C, where the average grain size may grow up to about 500 nm and more $MgZn_2$ precipitates can form along grain boundaries.

Tensile test

The mechanical tests of the alloy samples with a gauge part of $2.0 \times 1.0 \times 0.8$ mm were conducted at 150 °C ($0.45 \times T_m$) in the range of strain rate, $\dot{\varepsilon}$ of $10^{-4} \div 5 \times 10^{-3}\text{s}^{-1}$.

Impression creep test

For impression creep measurements, small disks having a thickness between 3 and 4 mm were cut from the billets. It is well-established that during an impression creep test a cylindrical flat-ended punch under constant load is pressed continuously into the surface of the sample. According to experimental evidence, the penetration velocity of the punch becomes constant (steady) after an initial transient. The impression creep process is then characterized by steady penetration of the punch [19, 27, 28]. In the present work, the impression creep measurements were performed on a device developed at the Department of Materials Physics, Eötvös Loránd

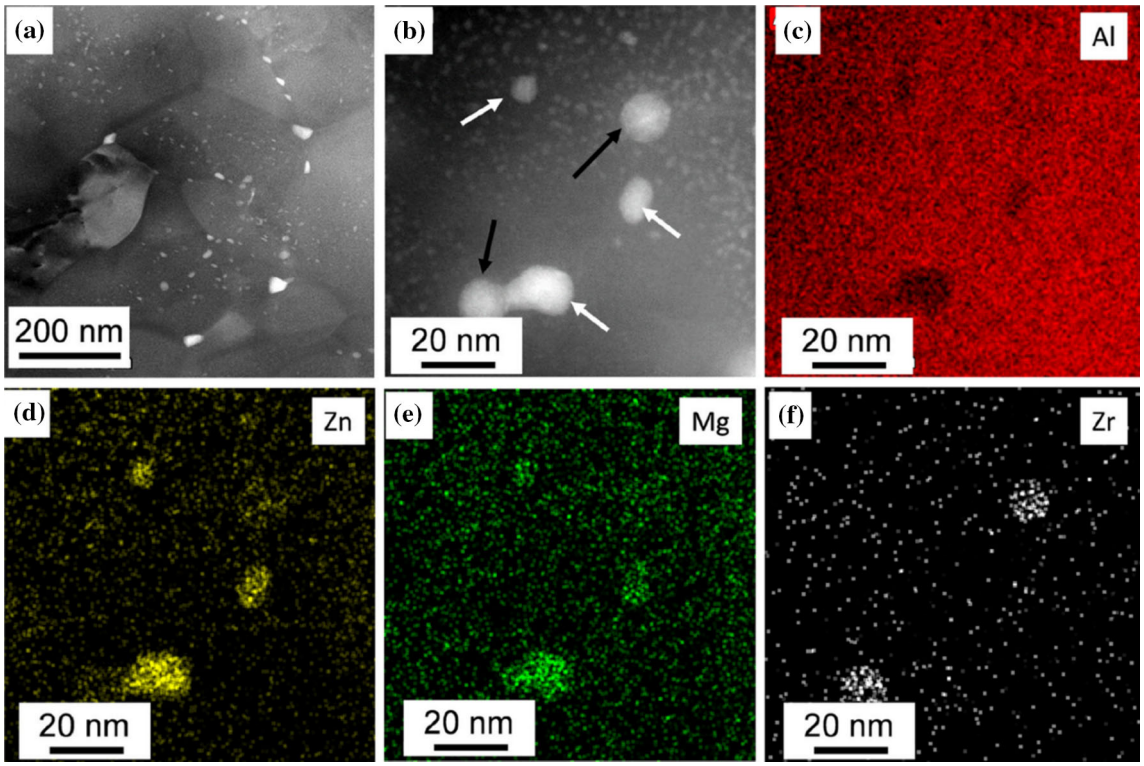

Figure 1 Ultrafine-grained microstructure of the investigated ECAP-processed AlZnMgZr sample taken as **a**, **b** HAADF STEM images in low and higher magnifications showing grains and precipitates, respectively, and **c**–**f** EDS elemental maps for Al, Zn, Mg, and Zr obtained on the area shown in (**b**). The white and black arrows in image **b** indicate Mg/Zn- and Zr-rich large precipitates. Reproduced from Ref. [4]. Copyright 2019, Springer.

University, Budapest. The impression was processed with a cylindrical punch having a diameter of $d = 0.5$ mm under different loads. The applied stress can be changed anytime during the measurement by changing the load. The furnace used for the test is precisely controlled by a computer, so the set temperature can be kept within ±1 °C (1 K) in the range between 100 and 200 °C, under $0.5T_m$. For measuring the displacement, a linear variable differential transformer (LVDT) is used with the resolution of 0.01 μm. The impression velocity (v_i) and the applied force (F) were converted into equivalent tensile stress (σ) and strain rate $(\dot{\varepsilon})$ using the following formulas:

$$\sigma = k_1 \frac{4F}{\pi d^2} \quad \text{and} \quad \dot{\varepsilon} = k_2 \frac{v_i}{d} \tag{1}$$

where $k_1 = 0.287$(often taken simply as 1/3) and $k_2 = 1$ are constant characteristics to the materials [20]. In the present work, the applied stress was in the range between 26 and 240 MPa, and the corresponding strain rate extended in the range from 2×10^{-6} to $5 \times 10^{-3}\text{s}^{-1}$.

Experimental results

Super ductility and low apparent strain rate sensitivity at low temperature

Figure 2a shows stress–strain curves of the samples deformed at different strain rates at 150 °C. It can be seen that the super ductility of almost 200% was observed at strain rate, $\dot{\varepsilon}$ of $10^{-4}s^{-1}$. This observation suggests a strain rate sensitivity higher than 0.3–0.35 should be characterizing the deformation of this UFG sample under the given conditions. As it has been mentioned, there is an unambiguous relationship between the ductility and the strain rate sensitivity (SRS) of the materials [16–18], and the total elongation of 100–200% can be expected at strain rate sensitivity higher than 0.3. In order to estimate the strain rate sensitivity, the double logarithm plot of stress and strain rate $(\ln\sigma - \ln\dot{\varepsilon})$ data obtained at constant strain having an elongation of 50% are given in Fig. 2b, where both local values for two close strain rates and the average value for the whole strain rate

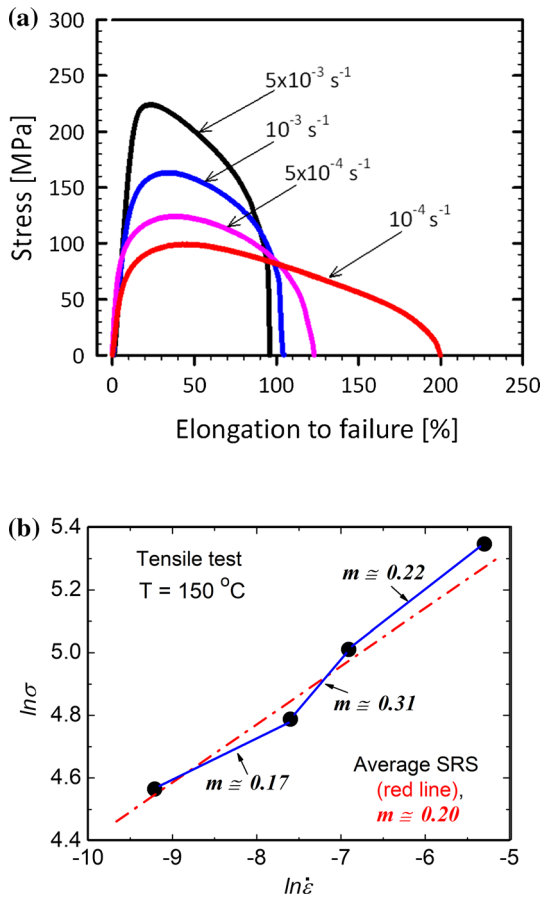

Figure 2 Characteristics of low temperature super ductility in the UFG Al–Zn–Mg–Zr alloy: **a** Stress–strain (σ–ε) curves, showing a total elongation of about 200% and **b** Logarithm of the stress ($\ln\sigma$) obtained at an elongation of 50% versus the logarithm of the strain rate ($\ln\,\dot{\varepsilon}$) for estimating the local and average apparent strain rate sensitivity (m parameter).

range, according to the $m = \left(\frac{\partial \ln \sigma}{\partial \ln \dot{\varepsilon}}\right)_{\varepsilon}$ definition, can be seen.

Experimental results show that in spite of relatively high elongation, the strain rate sensitivity seems to be low, of only about 0.2. Especially, the local value at lowest strain rate – and then at the lowest stress – is only 0.17. In order to clarify the contradictory situation, more details were analyzed by using impression creep measurements.

Threshold stress of deformation process

Impression creep tests were performed at 140, 150 and 160 °C. The experimental results show that the impression velocity, v_i – when the creep takes place—is strongly temperature- and load-dependent, indicating that the deformation process is thermally activated, and the flow rate is strongly stress-dependent. However, at each testing temperature it seems that the creep process only starts above a certain stress (load), as shown, for example, in Fig. 3, where the impression depth, h is plotted as the function of time, t for two different stresses at the testing temperature of 150 °C. It can be seen that the impression process took place at $\sigma = 67$MPa, with a small, steady velocity, v_i of about $9 \times 10^{-4}\mu m/\mathrm{s}$, resulting in a strain rate, $\dot{\varepsilon}$ of about $2 \times 10^{-6}\mathrm{s}^{-1}$. However, the creep process could not start at all at lower $\sigma = 26MPa$. This experimental experience is referring to the existence of a threshold stress, σ_0 at a given testing temperature.

Analyzing the experimental data including a threshold stress

Considering the general experience mentioned above, the creep process at a given temperature, T is described in terms of effective stress, $\sigma_{\mathrm{eff}} = \sigma - \sigma_0$ instead of the applied stress, σ by the following rate equations:

$$\dot{\varepsilon} = A\sigma_{\mathrm{eff}}^{1/m}\exp(-Q/RT), \quad \text{or}$$
$$\dot{\varepsilon} = A(\sigma - \sigma_0)^{1/m}\exp(-Q/RT) \qquad (2)$$

where A is a material constant, m is the strain rate sensitivity parameter (the term $1/m$ is often called as stress exponent), Q is the activation energy of the creep process, R is the universal gas constant and the testing temperature, T is given in Kelvin. It should be noted that the concept is to use Eq. (2) was successfully applied for the description of the creep process of several materials [22, 32, 33].

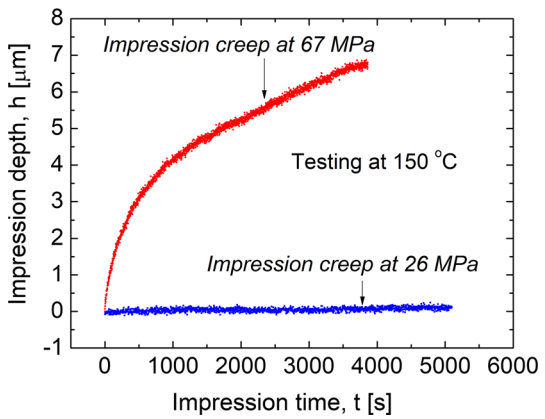

Figure 3 Impression depth-time (h–t) taken at different stresses, referring to the existence of a threshold stress, σ_0.

In order to determine, strain rate sensitivity, m and the activation energy, Q– the main characteristics of the deformation process – let us rewrite Eq. (2) as

$$\dot{\varepsilon}^m = A^m(\sigma - \sigma_0)\exp(-mQ/RT), \quad \text{or}$$
$$\sigma = \sigma_0 + \frac{1}{A^m}\exp\left(\frac{mQ}{RT}\right)\dot{\varepsilon}^m \tag{3}$$

showing a linear function between σ and $\dot{\varepsilon}^m$ quantities. In the absence of the threshold stress ($\sigma_0 = 0$), we would regain the often used direct proportionality between σ and $\dot{\varepsilon}^m(\sigma - \dot{\varepsilon}^m)$, where the value of m could be determined simply from the slope of the double logarithmic $\ln\sigma - \ln\dot{\varepsilon}$ relationship.

Considering also the existence of the threshold stress, σ_0, the strain rate sensitivity can be determined by choosing the value of m as a best-fit parameter for linear fitting to the data in an $\dot{\varepsilon}^m - \sigma$ plot at a given testing temperature. Figure 4 shows such best fits at different testing temperatures. The best-chosen values of m were 0.33, 0.32, and 0.35 for the temperatures of 140, 150 and 160 °C, giving the values of σ_0 as 57, 54 and 53 MPa, respectively. Considering also the error of the measurements, a value of 0.33 ± 0.02 can be regarded as the strain rate sensitivity of the investigated sample. This relatively high strain rate sensitivity parameter is confirming the super ductility of the investigated ultrafine-grained AlZnMgZr material at the low testing temperatures under $0.5T_m$. It should be noted that when aging at the temperature range between 120 and 170 °C [4], more intermetallic η-$MgZn_2$ precipitates are formed in the grain boundaries due to the accelerated grain boundary diffusion. Although further investigations are needed to clarify the origin of the threshold stress, it can be supposed that this origin is certainly connected to the existence of the incoherent η-$MgZn_2$ precipitates during the deformation process taken by grain boundary sliding in a UFG material.

Taking into account the threshold stress, the $\ln\sigma_{\text{eff}} - \ln\dot{\varepsilon}$ relationships for impression creep tests taken at different testing temperatures are shown in Fig. 5, where – for comparison – the experimental data obtained for the tensile test (shown in Fig. 2b) can also be seen, using the threshold stress of 54 MPa for the testing temperature of 15 °C. In addition to the clearly visible linearity of the $\ln\sigma_{\text{eff}} - \ln\dot{\varepsilon}$ relationships, giving a strain rate sensitivity of 0.33 ± 0.02, it is also clear that the data obtained at 150 °C by the two methods show a good agreement, confirming the validity of the indentation procedure.

Considering Eq. (3), it can be seen that the slope, C^* of the linear line – shown in Fig. 4—fitted to the $\dot{\varepsilon}^m - \sigma$ data obtained at temperature T is depending on the testing temperature as:

$$C^* = \frac{1}{A^m}\exp\left(\frac{mQ}{RT}\right),$$

from which we have:

$$\ln C^* = -m\ln A + \frac{mQ}{RT} \tag{4}$$

According to Eq. (4), the value of activation energy, Q can be determined from the slope of the linear line fitted to the $lnC^* - \frac{1}{T}$ data, as shown in Fig. 6. Here we have to use the value of the universal gas constant, $R = 8.31\frac{J}{\text{mole}\cdot K}$, and the value of strain rate sensitivity, $m = 0.33$.

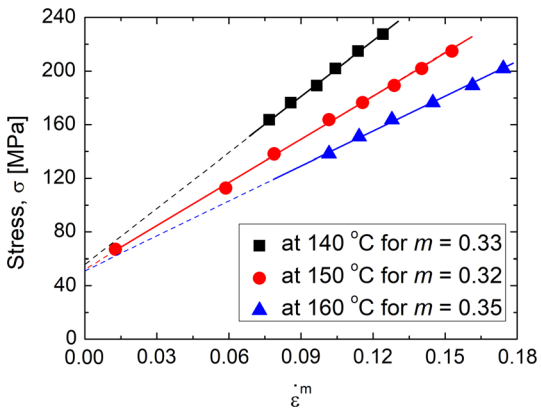

Figure 4 The $\dot{\varepsilon}^m - \sigma$ functions with the best-chosen m-value for linear connections at different testing temperatures.

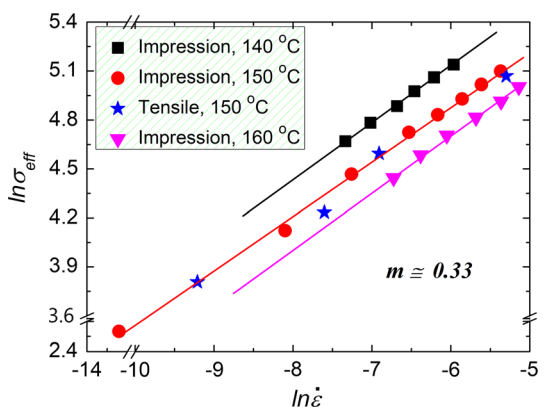

Figure 5 The $\ln\sigma_{\text{eff}} - \ln\dot{\varepsilon}$ relationships for impression creep tests at different testing temperatures and for tensile test at 150 °C.

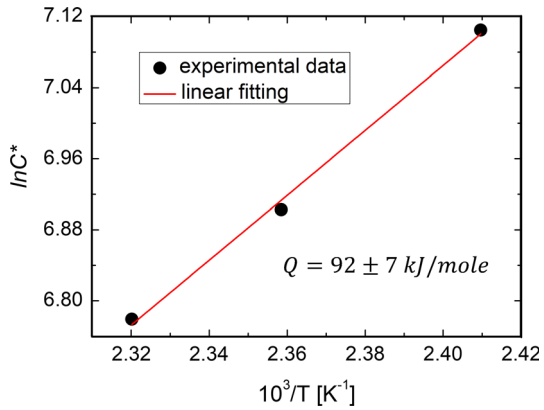

Figure 6 Determination of the activation energy, Q using Eq. (4) with data obtained from Fig. 4.

Experimental results show that the activation energy of the investigated UFG alloy is $Q = 92 \pm 7$kJ/mole. This experimentally determined value is much lower than the value for self-diffusion in pure Al (142 kJ/mole [34]). In the lower temperature region under $0.5T_m$, a significant effect of lattice diffusion cannot be expected. This is also the reason for the stability of the UFG microstructure. The obtained activation energy is rather similar to the value for grain boundary diffusion in pure Al (84 kJ/mole [34]) and may suggest that the basic mechanism of the low temperature deformation process in this UFG material is also grain boundary sliding, similarly to that of high temperature superplasticity. However, the experimentally obtained strain rate sensitivity of 0.33 (or its reciprocal, the so-called stress exponent having a value of 3) suggests a possible control by a viscous glide process [35]. Further investigations are needed to look in more detail at direct evidence for viscous glide and/or grain boundary sliding, clarifying the effect of the thermally activated process in this complex composition UFG AlZnMgZr alloy, processed by ECAP. It should also be mentioned that the same composition UFG alloy processed by HPT [9] can be deformed superplastically at 150 °C, for a maximum elongation of 400%, which is twice that of the present ECAP-processed sample. Understanding this significant difference will also be the aim of the mentioned further studies.

Conclusions

Characteristics of low temperature plastic deformation of an ECAP-processed ultrafine-grained AlZnMgZr alloy were studied by tensile and impression creep tests in the low temperature region between 140 and 160 °C. The main results can be summarized as follows:

(1) It was demonstrated that this UFG alloy shows super ductility at low temperatures, as it can be deformed for maximum elongation of ~ 200% at 150 °C.

(2) It has been shown that threshold stress should be considered in the description of the deformation process, which can be characterized by the strain rate sensitivity of $\sim 0.33 \pm 0.02$ and activation energy of $\sim 92 \pm 7$kJ/mole.

(3) These experimentally determined parameters confirm the potential for superplasticity of the investigated UFG alloy at low temperatures, below half of the absolute melting point ($0.5T_m$). The obtained results are important not only in the basic research but also in the economical application of fine-grained materials.

Acknowledgements

The present research was financed by the Hungarian-Russian bilateral Research program (TÉT) No. 2017-2.3.4-TÉT-RU-2017-00005. This work was completed in the ELTE Institutional Excellence Program (TKP2020-IKA-05) financed by the Hungarian Ministry of Human Capacities. The research of B.B. was also supported by the ÚNKP-19-2 New National Excellence Program of the Ministry for Innovation and Technology. R.Z.V. and M.Y.M. acknowledge the support from the Ministry of Science and Higher Education of the Russian Federation under grant agreement No. 0838-2020-0006.

Funding

Open access funding provided by Eötvös Loránd University.

Data availability

The data that support the findings of this study are all the own results of the authors, not available anywhere.

Declarations

Conflict of interest The authors declare that they have no conflict of interest.

References

[1] Valiev RZ, Langdon TG (2006) Principles of equal channel angular pressing as a processing tool for grain refinement. Prog Mater Sci 51:881–981

[2] Gubicza J, Schiller I, Chinh NQ, Illy J, Horita Z, Langdon TG (2007) The effect of severe plastic deformation on precipitation in supersaturated Al–Zn–Mg alloys. Mater Sci Eng A 460–461:77–85

[3] Chinh NQ, Gubicza J, Czeppe T, Lendvai J, Xu C, Valiev RZ, Langdon TG (2009) Developing a strategy for the processing of age-hardenable alloys by ECAP at room temperature. Mater Sci Eng A 516:248–252

[4] Gubicza J, Lábár JL, Lendvai J, Chinh NQ (2019) The influence of artificial aging on the microstructure and hardness of an Al–Zn–Mg–Zr alloy processed by equal channel angular pressing. J Mater Sci 54:10918–10928

[5] Duan ZC, Chinh NQ, Xu C, Langdon TG (2010) Developing processing routes for the equal-channel angular pressing of age-hardenable aluminum alloys. Metall Mater Trans 41A:802–809

[6] Kawasaki M, Langdon TG (2016) Review: achieving superplastic properties in ultrafine-grained materials at high temperatures. J Mater Sci 51:19–32. https://doi.org/10.1007/s10853-015-9176-9

[7] Zhilyaev AP, Langdon TG (2008) Using high-pressure torsion for metal processing: fundamentals and applications. Prog Mater Sci 53:893–979

[8] Gubicza J, El-Tahawy M, Lábár JL, Bobruk EV, Murashkin MYu, Valiev RZ, Chinh NQ (2020) Evolution of microstructure and hardness during artificial aging of an ultrafine-grained Al–Zn–Mg–Zr alloy processed by high pressure torsion. J Mater Sci 55:16791–16815. https://doi.org/10.1007/s10853-020-05264-4

[9] Valiev RZ, Kazykhanov VU, Mavlyutov AM, Yudakhina AA, Chinh NQ, My M (2020) Superplasticity and high-strength in Al–Zn–Mg alloy with Ultrafine grains. Adv Eng Mater 22(1):1900555

[10] Chinh NQ, Valiev RZ, Sauvage X, Varga G, Havancsák K, Kawasaki M, Straumal BB, Langdon TG (2014) Grain boundary phenomena in an ultrafine-grained Al–Zn alloy with improved mechanical behavior for micro-devices. Adv Eng Mater 16:1000–1009

[11] Valiev RZ et al (2010) Unusual super-ductility at room temperature in an ultrafine-grained aluminum alloy. J Mater Sci 45:4718–4724. https://doi.org/10.1007/s10853-010-4588-z

[12] Hall EO (1951) The deformation and ageing of mild steel: III discussion of results. Proc Phys Soc B 64:747–753

[13] Petch NJ (1953) The cleavage strength of polycrystals. J Iron Steel Inst 174:25–30

[14] Chinh NQ, Szommer P, Horita Z, Langdon TG (2006) Experimental evidence for grain boundary sliding in ultrafine-grained aluminum processed by severe plastic deformation. Adv Mater 18:34–39

[15] Chinh NQ, Szommer P, Gubicza J, El-Tahawy M, Bobruk EV, My M, Valiev RZ (2020) Characterizing microstructural and mechanical properties of Al–Zn alloys processed by high-pressure torsion (review paper). Adv Eng Mater 22(1):1900672

[16] Woodford DA (1969) Strain-rate sensitivity as a measure of ductility. Trans ASM 62:291–293

[17] Langdon TG (1982) The mechanical properties of superplastic materials. Metall Trans 13A:689–701

[18] Chinh NQ, Rácz G, Gubicza J, Valiev RZ, Langdon TG (2019) A possible stabilizing effect of work hardening on the tensile performance of superplastic materials. Mater Sci Eng A 759:448–454

[19] Chu SNG, Li JCM (1977) Impression creep; a new creep test. J Mater Sci 12:2200–2208. https://doi.org/10.1007/BF00552241

[20] Yu HY, Imam MA, Rath BB (1985) Study of the deformation behavior of homogeneous materials by impression tests. J Mater Sci 20:636–642. https://doi.org/10.1007/BF01026536

[21] Tasnádi P, Juhász A, Chinh NQ, Kovács I (1988) Theoretical description of the defomation taking place in an impression test. Res Mech 24:335–347

[22] Chinh NQ, Tasnádi P, Juhász A, Kovács I, Kovács Csetényi E (1994) Evaluation of the true activation enthalpy of superplastic flow including a threshold stress. J Mater Sci 29:2341–2343. https://doi.org/10.1007/BF00363424

[23] Chinh NQ, Ily J, Juhász A, Lendvai J (1995) Mehanical properties and superplasticity of AlZnMg alloys with copper and zirconium additions. Phys Stat Sol (A) 149:583–592

[24] Chinh NQ, Juhász A, Tasnádi P, Kovács I, Kovács-Csetényi E (1996) The existence of the threshold stress in superplastic Al alloys. J Mat Sci Lett 15:406–408

[25] Cseh G, Chinh NQ, Tasnádi P, Szommer P, Juhász A (1997) Indentation test for the investigation of plasticity of glasses. J Mat Sci 32:1733–1739

[26] Cseh G, Chinh NQ, Tasnádi P, Szommer P, Juhász A (1997) Indentation test for the investigation of high temperature plasticity of materials. J Mat Sci 32:5107–5111

[27] Li JCM (2002) Impression creep and other localized tests. Mater Sci Eng A 322:23–42

[28] Sastry DH (2005) Impression creep technique—An overview. Mater Sci Eng A 409:67–75

[29] Talari MK, Babu NK, Kallip K, Leparoux M, Koller RE, Alogab KA, Maeder X (2016) Microstructure, mechanical, and impression creep properties of AlMg5–0.5 vol% Al_2O_3 Nanocomposites. Adv Eng Mater 18:1958–1966

[30] Wang H, Wang QD, Boehlert CJ, Yang J, Yin DD, Yuan J, Ding WJ (2016) The impression creep behavior and microstructure evolution of cast and cast-then-extruded Mg–10Gd–3Y–0.5Zr (wt%). Mater Sci Eng A 649:313–324

[31] Kumar A, Ramteke S, Chelika S, Vanitha C (2021) Creep behavior of Al–Si–Mg alloy by hot impression creep test. Mater Today Proceed 41:1207–1211

[32] Burton B (1977) "Diffusional creep of polycrystalline materials", Diffusion and Defect Monograph Series. Trans. Tech, Switzerland

[33] Mohamed FA (1983) Interpretation of superplastic flow in terms of a threshold stress. J Mater Sci 18:582–592 https://doi.org/10.1007/BF00560647

[34] Frost HJ, Ashby MF (1982) Deformation-mechanism maps: the plasticity and creep of metals and ceramics. Pergamon Press, Oxford (UK)

[35] Mohamed FA, Langdon TG (1974) Transition from dislocation climb to viscous glide in creep of solid solution alloys. Acta Met 22:779–788